SARS-CoV-2 infection of thymus induces loss of function that correlates with disease severity

Marco Rosichini, MSc,[a,b]* Veronica Bordoni, PhD,[a,c]* Domenico Alessandro Silvestris, PhD,[a] Davide Mariotti, MSc,[c] Giulia Matusali, PhD,[d] Antonella Cardinale, MSc,[a] Giovanna Zambruno, MD,[e] Angelo Giuseppe Condorelli, PhD,[e] Sara Flamini, PhD,[a] Shirley Genah, PhD,[a] Marialuigia Catanoso, MD,[a,f] Franca Del Nonno, MD,[g] Matteo Trezzi, MD,[h] Lorenzo Galletti, MD,[h] Cristiano De Stefanis, MSc,[i] Nicolò Cicolani, BSc,[j] Stefania Petrini, PhD,[j] Concetta Quintarelli, PhD,[a,k] Chiara Agrati, PhD,[a,c]* Franco Locatelli, MD,[a,l]* and Enrico Velardi, PhD[a]*   *Rome, Italy*

GRAPHICAL ABSTRACT
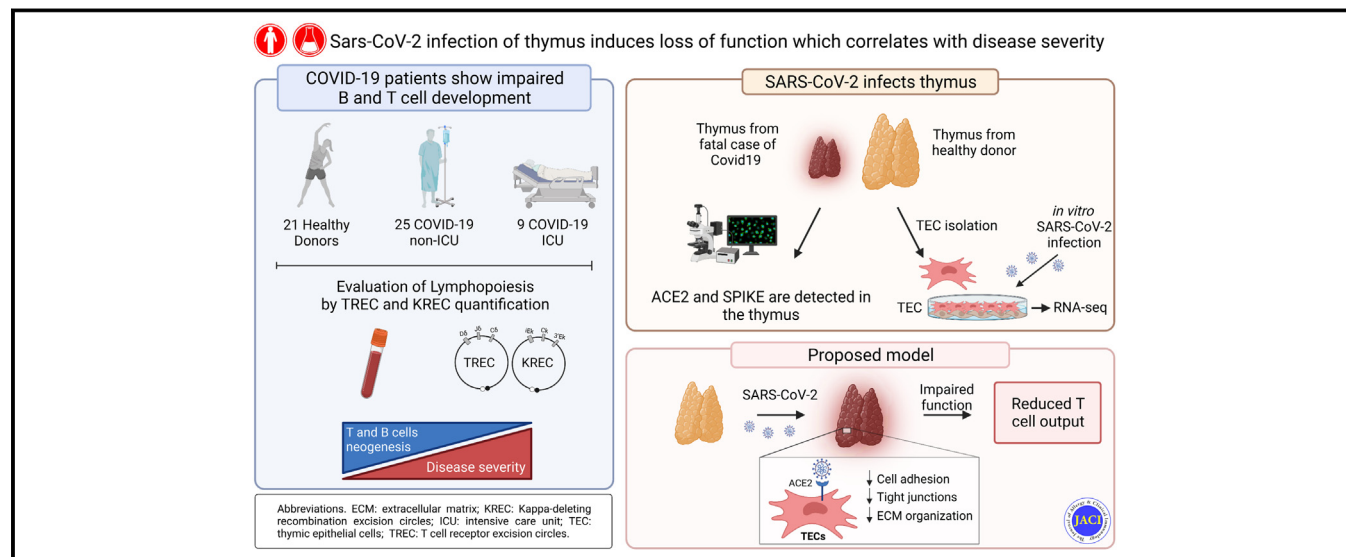
Background: Lymphopenia, particularly when restricted to the T-cell compartment, has been described as one of the major clinical hallmarks in patients with coronavirus disease 2019 (COVID-19) and proposed as an indicator of disease severity. Although several mechanisms fostering COVID-19–related lymphopenia have been described, including cell apoptosis and tissue homing, the underlying causes of the decline in T-cell count and function are still not completely understood.
Objective: Given that viral infections can directly target thymic microenvironment and impair the process of T-cell generation, we sought to investigate the impact of severe acute respiratory syndrome coronavirus 2 (SARS-CoV-2) on thymic function.
Methods: We performed molecular quantification of T-cell receptor excision circles and κ-deleting recombination excision circles to assess, respectively, T- and B-cell neogenesis in SARS-CoV-2–infected patients. We developed a system for *in vitro* culture of primary human thymic epithelial cells (TECs) to mechanistically investigate the impact of SARS-CoV-2 on TEC function.

Results: We showed that patients with COVID-19 had reduced thymic function that was inversely associated with the severity of the disease. We found that angiotensin-converting enzyme 2, through which SARS-CoV-2 enters the host cells, was expressed by thymic epithelium, and in particular by medullary TECs. We also demonstrated that SARS-CoV-2 can target TECs and downregulate critical genes and pathways associated with epithelial cell adhesion and survival.

Conclusions: Our data demonstrate that the human thymus is a target of SARS-CoV-2 and thymic function is altered following infection. These findings expand our current knowledge of the effects of SARS-CoV-2 infection on T-cell homeostasis and suggest that monitoring thymic activity may be a useful marker to predict disease severity and progression. (J Allergy Clin Immunol 2023;■■■:■■■-■■■.)

Since December 2019, a new infectious respiratory disease, named coronavirus disease 2019 (COVID-19) and caused by the severe acute respiratory syndrome coronavirus 2 (SARS-CoV-2), emerged in Wuhan, China, and spread worldwide, causing a pandemic. Apart from the respiratory tract, a large variety of organs and tissues are also affected by SARS-CoV-2 infection. Lymphopenia has been described as one of the major clinical hallmarks in infected patients and proposed as an indicator of disease severity.[1-3] Although transient lymphopenia is a common feature of many respiratory viral infections, it normally lasts 2 to 4 days, after which patients recover. By contrast, the lymphopenia observed in patients with COVID-19 appears to be more severe and persistent, as well as particularly selective for T-cell lineage.[4] Thus, multiple studies have investigated the underlying causes of the T-cell lymphopenia in patients with COVID-19 and its correlation with disease severity and progression. Exhaustion and depletion of T cells during COVID-19 progression have been attributed to several processes triggered by a highly inflammatory microenvironment, including aberrant activation, cell apoptosis, and tissue recruitment.[5-8]

The thymus gland is the primary organ for the generation and education of T cells. This process is highly dependent on the cross talk between developing thymocytes and the thymic stromal compartment, which consists of thymic epithelial cells (TECs), macrophages, endothelial cells, fibroblasts, and dendritic cells.[9-11] TECs account for most of the thymic stromal population and are classically divided into cortical and medullary TECs (cTECs and mTECs, respectively) according to their localization and functional properties.[11,12] cTECs control fate commitment, expansion, and positive selection of the developing thymocytes. mTECs are primarily involved in the negative selection of thymocytes and in the establishment of the "central tolerance" through the presentation of self-peptides restricted to organs in the periphery by the MHC. Thus, mTECs play a critical role in the induction of tolerance to a large array of tissue-restricted antigens.[13]

The process of T-cell development is severely altered by immunologic insults, such as those associated with common antineoplastic therapies (radiotherapy or chemotherapy), immunosuppressive treatments, and infections.[14] Viral and bacterial infections negatively affect thymic function through the direct targeting of cells of the thymic microenvironment or through

bystander systemic effects of soluble factors released in the bloodstream, such as glucocorticoids and proinflammatory cytokines.[15-19] Clinical and experimental evidence demonstrates that multiple viruses, such as HIV,[17,20-23] measles virus,[24,25] human T-lymphotropic virus type 1,[26,27] Zika virus,[28] chronic hepatitis C virus,[19] highly pathogenic avian influenza viruses,[29] and simian immunodeficiency virus,[30] affect the thymic local microenvironment and disrupt its function, leading to a reduction in T-cell neogenesis. Despite the detrimental effects of viral infections on thymic function, the very few studies analyzing T lymphopoiesis during SARS-CoV-2 infection have shown contrasting results.[31,32]

Here, we have hypothesized that SARS-CoV-2 can directly target cells in the thymus and affect its function. We provide compelling evidence that patients with COVID-19 display altered thymic function and that SARS-CoV-2 directly influences thymic epithelium function. We have demonstrated that patients with COVID-19 had severely reduced thymic T-cell output and that the disease severity was associated with a decline in thymic function. Mechanistically, we found that the angiotensin-converting enzyme 2 (ACE2), which is the main receptor for entry of SARS-CoV-2 into the host cells, was expressed in thymic epithelium and in particular by mTECs. We also demonstrated that SARS-CoV-2 can enter TECs and affect their gene expression profile, upregulating genes linked to the "coronavirus disease" and downregulating pathways associated with epithelial cell adhesion and survival.

Our results expand current knowledge of the effects of SARS-CoV-2 infection on patients' immune system and suggest that monitoring thymic activity might be a useful marker to evaluate disease severity and progression.

METHODS
Study design
A total of 34 hospitalized patients with COVID-19 were retrospectively enrolled in the study. The inclusion criterion was molecular diagnosis of SARS-CoV-2 infection confirmed by RT-PCR on nasopharyngeal swab. The

TABLE I. Patient demographic information

Study group	Healthy donors	COVID-19 (non-ICU)	COVID-19 (ICU)
Healthy subjects and patients, no.	21	25	9
Age (y), median (IQR)	49 (30-52)	59 (48-73)	57 (55-77)
Sex (M/F), no.	7/14	18/7	7/2
Day of analysis (d from admission), median (IQR)	N/A	1 (0-2)	2 (1-4)
Lymphocyte count (κ 10^9/L), mean ± SD	N/A	1.2 ± 0.7	1 ± 0.8

exclusion criteria were HIV, hepatitis B virus, hepatitis C virus infection, and pregnancy. Patients were further divided into 2 cohorts based on the severity of their disease: 9 patients were admitted to the intensive care unit (ICU), whereas 25 patients were not (non-ICU). A total of 21 adult healthy donors not infected with SARS-CoV-2 were enrolled in the control group (the healthy donor group). Patient demographic information is detailed in Table I.

This observational study was conducted on adult patients hospitalized at the INMI Lazzaro Spallanzani Hospital–IRCCS (Rome, Italy) from the beginning of March 2020 to the end of October 2020. Ethical approval was obtained from the ethics committee of INMI, Lazzaro Spallanzani (protocol approval no. 9/2020), and each patient signed a written informed consent form. The study was performed in accordance with the Good Clinical Practice guidelines, the International Conference on Harmonization guidelines, and the most recent version of the Declaration of Helsinki.

Generation of hTEC cultures

Cell cultures of primary human TECs (hTECs) were established following the procedure originally described by Green et al[33] with modifications. Thymus tissue samples were obtained during corrective cardiovascular surgery from pediatric patients after their parents signed a written informed consent form. Thymus capsule was removed to make the innermost lobules visible. Thymic specimens were finely minced and suspended in RPMI medium (Euroclone, Pero, Italy) containing 0.06 mg/mL of Liberase (Merck, Darmstadt, Germany), 0.4 mg/mL of DNAse from bovine pancreas (Roche, Basel, Switzerland), and 2 mM L-Glutamine (Euroclone) and rotated in spinner flasks at 37°C for 3 cycles of 20 minutes each. Digested specimens were collected in RPMI medium containing 2% FBS (ThermoFisher Scientific, Waltham, Mass), pooled, and spun at 300 g for 5 minutes at 4°C. To enrich for TECs, epithelial cell adhesion molecule (EpCAM)-positive cells were enriched by using anti-EpCAM (CD326) (clone HEA-125, Miltenyi, Bergisch Gladbach, Germany) staining and anti-APC microbeads (Miltenyi) separation. The TEC-enriched cell fraction was plated (2.5×10^4 cells/cm^2) on a feeder layer of lethally irradiated 3T3-J2 murine fibroblasts (Kerafast, Boston, Mass) and cultured in a humidified atmosphere of 5% CO_2 in growth medium composed of a mixture of Dulbecco modified Eagle medium and Ham's F-12 (a 3:1 mixture), 10% FCS (ThermoFisher Scientific), insulin (5 μg/mL, Eli Lilly, Indianapolis, Ind), adenine (0.18 mM, Sigma, St Louis, Mo), hydrocortisone (0.4 μg/mL, Sigma), cholera toxin (0.1 nM, List Labs, Campbell, Calif), triiodothyronine (2 nM, Sigma), glutamine (4 mM, ThermoFisher Scientific), and antibiotics. Epidermal growth factor (10 ng/mL, Austral Biologicals, San Ramon, Calif) was added to medium after 48 hours of culture. Cultured TECs were assessed by standard light sheet microscopy for the maintenance of TEC-like morphology and by fluorescence-activated cell sorting for expression of the TEC markers EpCAM, Ulex europaeus agglutinin I (UEA1, clone GoH3, DBA), and CD205 (clone C205, BD, Franklin Lakes, NJ) to discriminate between mTECs (CD205^{low} UEA1^{high}) and cTECs (CD205^{high} UEA1^{low}). Twenty-four hours before the start of the experiments, hTECs were plated in KGM-Gold defined medium (Lonza, Basel, Switzerland) in the absence of feeder layer.

SARS-CoV-2 infection of TECs

hTECs were either not infected or infected with SARS-CoV-2 (SARS-CoV-2/Human/ITA/PAVIA10734/2020, clade G, D614G [S] Ref-SKU: 008V-04005, from the EVAg portal) in minimum essential medium at a multiplicity of infection of 1. Viral inoculum or medium only (not infected) was applied, and cells were incubated for 90 minutes at 37°C in 5% CO_2. Viral inoculum was then removed, and the cells were washed 2 times with 0.3 mL of PBS. The hTECs were fixed in paraformaldehyde 4% for immunofluorescence or lysed for gene expression analysis at the indicated time points after infection.

Viral RNA quantification

For viral RNA quantification, real-time RT-PCR was performed on 40 ng of cell-associated RNA by using the RealStar-SARS-CoV-2 RT-PCR Kit (Altona Diagnostics, Hamburg, Germany), which amplifies the E- and S- viral genes. A 5-point standard curve (10^6-10^2 SARS-CoV-2 RNA copies per reaction; Human 2019-nCoV strain 2019-nCoV/Italy-INMI1 RNA; Ref-SKU: 008N-03894, from EVAg portal) was run in parallel with experimental samples in each RT-PCR.

Immunofluorescence

For the in vitro experiments with hTECs, cells were fixed in paraformaldehyde 4% after SARS-CoV-2 infection, washed 3 times with PBS for 5 minutes, and blocked with blocking buffer (2% goat serum from Invitrogen, 1% BSA from Sigma Aldrich, 0.1% fish gelatin blocking agent from Biotium (Fremont, Calif), and 0.1% Triton X-100 and 0.05% Tween20 from Sigma Aldrich in PBS) for 1 hour at room temperature. After washing, the primary antibodies anti–Zonula occludens-1 (anti-ZO-1) (Invitrogen, Waltham, Mass) and anti–SARS-CoV-2 SPIKE (clone 1A9, GeneTex, Irvine, Calif) in primary antibody buffer (1% BSA and 0.1% fish gelatin blocking agent in PBS) were added and incubated overnight at 4°C in the dark. After washing, secondary antibodies (anti-mouse IgG1 Alexa-488 and anti-rabbit IgG Alexa-647 from Sigma Aldrich) were added to each condition and incubated for 2 hours at room temperature. After washing, the slides were mounted with SlowFade Gold Antifade Mountant with 4',6-diamino-2-phenylindole (Invitrogen). The images were acquired with a Leica THUNDER 3D Live Cell Imaging system using THUNDER Computational Clearing Settings at ×63 magnification.

For the evaluation of ACE2, SPIKE protein, cytokeratin 1 (CK1), and cytokeratin 5 (CK5) expression on human thymic samples, immunofluorescence analysis was performed on 2.5-μm-thick sections obtained from formalin-fixed paraffin-embedded tissues. After dewaxing and rehydrating, heat-induced epitope retrieval was performed by boiling the slides with EDTA (pH 9) (Dako, Santa Clara, Calif).

We tested the specificity of ACE2 antibody in testis, a tissue with a high level of ACE2 expression,[34] by using immunohistochemistry and immunofluorescence techniques.

For the immunohistochemistry, the epitope retrieval was performed by incubating the sections at room temperature with proteinase K (S3020) (Dako). Endogenous peroxidase was blocked with 3% hydrogen peroxide followed by another blocking step in 5% BSA. Sections were incubated overnight at 4°C with the anti-ACE2 antibody (dilution 1:500). Secondary biotinylated antibody (K8024, Dako) and the peroxidase DAB kit (Dako) were used to reveal the primary antibody. Hematoxylin and eosin staining was also performed following the standard procedure. Next, stained sections were acquired by using a digital scanner platform (Nanozoomer 2.0, Hamamatsu, Shizuoka, Japan).

For the immunofluorescence, after blocking in 5% BSA for 1 hour, tissue sections were incubated overnight at 4 °C with ACE2, SPIKE, CK1, or CK5

(dilution 1:100). The primary antibody was revealed with the secondary antibody Alexa Fluor goat anti-rabbit 555 or anti-mouse IgG1 Alexa-488 (Applied Biosystems, Waltham, Mass). For nuclear staining, HOECHST was added for 5 minutes before section mounting with glycerol/PBS (1:1). The images were acquired using a Leica TCS SP8X laser scanning confocal microscope (Leica Microsystems, Wetzlar, Germany) equipped with a white light laser source tunable in the range of 470 to 670 nm, a 405-nm diode laser, 3 photomultiplier tubes, and 2 internal spectral detector channels (HyD) GaAsP. Sequential confocal images using excitation spectral laser lines at 405 nm, 488 nm, and 555 nm were acquired by using C PLAN 10×/0.40 dry and HC PL APO CS2 63×/1.40 oil immersion objectives (Leica Microsystems) with a 1024 × 1024 format and scan speed of 200 Hz, with an electronic zoom up to 4×. The total number of ACE2- and cytokeratin-positive cells (CK1 or CK5) was counted in 3 to 4 digital confocal images randomly selected and analyzed for each tissue sample by 2 independent operators.

RNA-sequencing and bioinformatics analysis

Total RNA was extracted from primary cells with an RNeasy Plus Micro Kit (Qiagen, Hilden, Germania) according to the manufacturer's instructions. Samples were derived from 4 (at 24 hours) and 3 (at 48 hours) independent experiments using 3 biologic replicates. Quality control was performed through TapeStation 4200 and NanoDrop 2000c. Libraries were created (TruSeq stranded mRNA, Illumina, San Diego, Calif), and paired-end sequencing was performed with the Illumina platform. In the preprocessing step, the raw reads in fastq format were inspected and cleaned using FASTP.[35] The mean quality per base was fixed at a phred score of 20 and reads with more than 30% of unqualified bases (-q 20 -u 30 -l 55 –detect_adapter_for_pe) were removed. Reads shorter than 55 bases were also removed. Cleaned reads were aligned with STAR (2.7.9a)[36] using the ENCODE standard options onto a consensus version of the reference human genome (GRCh38). The 1000 Genomes Project variant call format file with consensus single-nucleotide variants and insertion/deletions (InDels) were provided at the genome generation stage and the alternative alleles in this variant call format have been inserted into the reference genome to create a "transformed" genome. At the mapping stage, the reads were mapped to the transformed genome and the alignments were transformed back to the original (reference) coordinates. Reads unmapped against the human genome were collected and realigned with Burrows-Wheeler Aligner (0.7.17) minimum essential medium onto the SARS-CoV-2 reference genome (NC_045512v2) using the default parameters. Gene expression was quantified with featureCounts[37] using the Gencode (release 42) reference gene annotation taking advantage of the strand-oriented nature of the reads. The list of human protein–coding genes linked to SARS-CoV-2 infection and COVID-19 disease was obtained from the Gencode database (https://www.gencodegenes.org/human/covid19_genes.html). The row counts were normalized with DESeq2[38] (1.38.1), and a batch effect correction was introduced with the R limma package.[39] Heatmaps were generated with the R *ComplexHeatmap* library, also highlighting clusters of coregulated genes. Differential gene expression analysis was conducted with DESeq2. The volcano plots were generated with the R *EnhancedVolcano* library. Gene set enrichment was tested with the EnrichR web tool (available at: https://maayanlab.cloud/Enrichr/). The RNA sequencing data have been deposited in the NCBI Sequence Read Archive (SRA) under ID: SRP422324.

Flow cytometry and cell sorting

For viability quantification, hTECs were stained with Fixable Viability Stain 440 UV (BD, catalog no. 566332) according to the manufacturer's instructions. Cells were then fixed with the Intracellular Fixation and Permeabilization buffer set (catalog no. 88-8824-00, eBioscience, San Diego, Calif). For surface marker analysis, cells were stained with fluorochrome-conjugated antibodies to identify TEC subsets. The antibodies used were as follows: CD326 (EpCam) (Miltenyi Biotec, catalog no. 130-113-822) and UEA1 (catalog no. FL-1061, DBA, Segrate, Italy). Acquisition was performed on a BD LSRFortessa X-20 (BD Biosciences), and data were analyzed with FlowJo version 8 (Treestar). For sorting of thymocytes, thymii from pediatric healthy donors were smashed on a 100-μm cell strainer to obtain total thymocytes. Cells were stained with fluorochrome-conjugated antibodies: CD3 (BD, catalog no. 565119), CD4

TABLE II. Probe and primer list

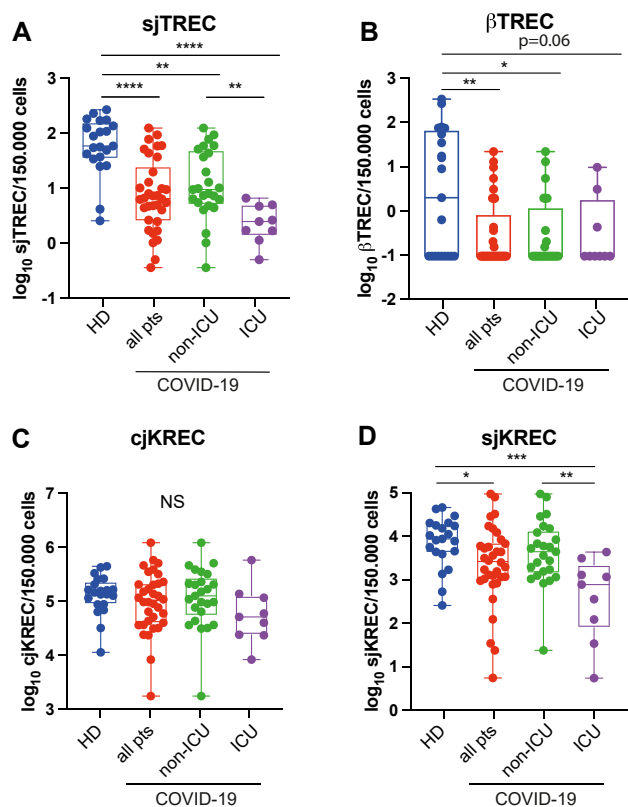| Target	Primer/probe
Albumin	FAM-CCTGTCATGCCCACACAAATCTCTCC-TAMRA
Db1	FAM-CAAAAACCTCTCTGGCGGTCCCAAC-TAMRA
Db2	FAM-CCCACCCAGCTCAGGGAATGCA-TAMRA
sjTREC	FAM-ACACCTCTGGTTTTTGTAAAGGTGCCCACT-TAMRA
cjKREC	FAM-AGCTGCATTTTTGCCATATCCACTATTTGGAGT-TAMRA
sjKREC	FAM-CCAGCTCTTACCCTAGAGTTTCTGCACGG-TAMRA
Albumin-F	GCTGTCATCTCTTGTGGGCTGT
Albumin-R	ACTCATGGGAGCTGCTGGTTC
Db1-in	TGTGACCCAGGAGGAAAGAAG
1.1-in	TGTCCTCCATCCTAGCCAGG
1.2-in	TCCGTCACAGGGAAAAGTGG
1.3-in	TGTCCCTGTGAGGGAAGAGTT
1.4-in	TGGACTTGGGGAGGCAGGA
1.5-in	CTCATAAAATGTGGGTCAGTGGA
1.6-in	TGAATCCAGGCAGAGAAAGG
Db2-in	GGACCAGCCCCAGAGAA
2.1-in	CCAGCTAACTCGAGACAGGAA
2.2-in	GAACCCTGTTCTTAGGGGAGT
2.3-in	TGAGAGGGGCTGTGCTGAGA
2.4-in	AAGCGGGGGCTCCCGCTGAA
cjKREC-F	CCCGATTAATGCTGCCGTAG
cjKREC-R	CCTAGGGAGCAGGGAGGCTT
sjKREC-F	TCAGCGCCCATTACGTTTCT
sjKREC-R	GTGAGGGACACGCAGCC

(BD, catalog no. 563876), and CD8 (BD, catalog no. 557746). 7-Aminoactinomycin D (7aad) (BD, catalog no. 559925) was used to assess cell viability. Cells were sort-purified using a BD Aria III cell sorter. The level of cell purity was greater than 98%.

TREC and KREC quantification

Genomic DNA was extracted from PBMCs with a Quick-gDNA Miniprep Kit (Zymo Research, Irvine, Calif), according to the manufacturer's instructions. T-cell receptor excision circles (TRECs) and κ-deleting recombination excision circles (KRECs) were quantified to evaluate T- and B-cell neogenesis, as previously described.[40-42] Briefly, a first PCR reaction was carried out with a primer mix containing primers, 0.5 to 1 μg of genomic DNA, 200 μM each 2′-deoxynucleoside 5′-triphosphate (dNTP), 2.5 mM MgCl₂, 1× buffer, and 1.25 U of platinum Taq polymerase (ThermoFisher) in 20 μL (3 minutes at 95°C followed by 18 cycles of 95°C for 15 seconds, 60°C for 30 seconds, and 68°C for 30 seconds). Quantification was made on a QuantStudio 12K Flex real-time PCR system, in duplicate with a second reaction containing 4 μL of a 1/200 or 1/2000 dilution of the first PCR product; primer; and probes for albumin, signal joint (sj) TRECs (sjTRECs), coding joint (cj) KRECs (cjKRECs), sjKRECs, or 1 of the Dβ-Jβ segments, Takyon Low Rox master mix (Eurogentec, Seraing, Belgium) in a final volume of 10 μL (40 cycles of 95°C for 15 seconds and 60°C for 1 minute). The sum of the 10 Dβ-Jβ segments was finally multiplied by 1.3 to extrapolate for all of the 13 existing Dβ-Jβ segments. Values were normalized for the genomic copy number by using albumin gene quantification. Data were expressed per 150,000 PBMCs. All primers and probes were purchased from Merck (Table II).

Statistics

Bars and error bars represent the mean plus or minus SEM for the various groups. For most experiments, nonparametric testing was performed if a normal distribution could not be assumed. Statistical analysis between 2 groups was
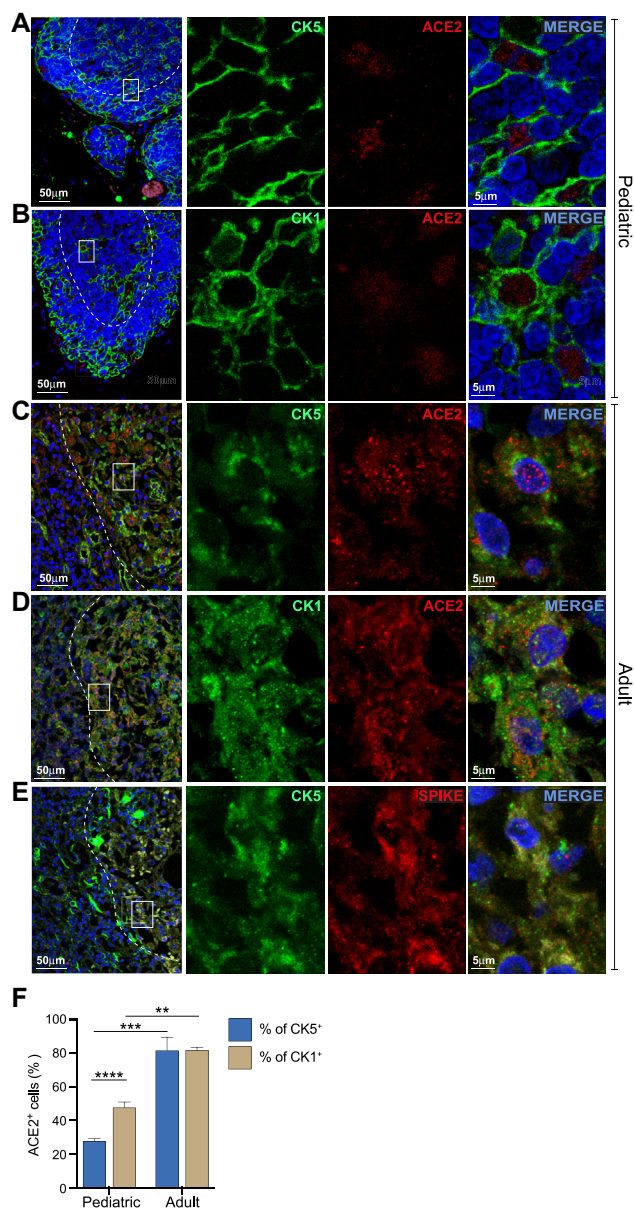
FIG 1. T- and B-cell neogenesis is impaired in patients (pts) with COVID-19. sjTREC (**A**) and βTREC (**B**) quantification per 150,000 cells. cjKREC (**C**) and sjKREC (**D**) quantification per 150,000 cells. Analyses include data on 21 healthy donors (HD), 25 non-ICU pts, and 9 ICU pts. *$P < .05$; **$P < .01$; ***$P < .001$; ****$P < .0001$. *NS,* Not significant.

performed with the nonparametric, unpaired Mann-Whitney *U* test. In general, variation within groups and between experiments was low; however, to take into account interexperimental variation, all experiments were performed at least twice. To account for intraexperimental variation, particularly for *in vitro* studies, multiple wells per condition were assessed with primary sample material coming from at least 2 different thymus tissue samples. All statistics were calculated, and display graphs were generated using GraphPad 9.

RESULTS

T- and B-cell neogenesis is impaired in patients with COVID-19

To assess the impact of COVID-19 on the process of T-cell development, we quantified TRECs in patient peripheral blood, a well-defined strategy to measure thymic T-cell neogenesis.[40-42] We specifically assessed sjTRECs and β-TRECs (βTRECs), which represent episomal DNA molecules generated during the intrathymic VDJ recombination of the T-cell receptor-α and -β locus, respectively.[43] The patients with COVID-19 showed significantly reduced thymic functionality, as demonstrated by the reduction in the levels of sjTRECs when compared with the levels in age-matched healthy controls (Fig 1, *A*). Importantly, the ICU patients showed a more dramatic reduction in sjTREC number when compared with the number in the non-ICU cohort, suggesting a more severe impairment of thymic function in patients with life-threatening disease (Fig 1, *A*). Despite the fact that βTRECs are canonically less detectable in the peripheral blood than are

FIG 2. Human thymus is a direct target of SARS-CoV-2 infection. ACE2 expression in combination with CK5 (**A**) or CK1 (**B**) in pediatric thymus. ACE2 expression in combination with CK5 (**C**) or CK1 (**D**) in adult thymus isolated from a patient with a fatal case of COVID-19. **E,** SPIKE expression in combination with CK5 in adult thymus isolated from a patient with a fatal case of COVID-19. **F,** Quantification of ACE2 and CK5 as well as ACE2 and CK1 coexpression in cells of the medullary compartment (n > 3 fields per image). White dotted lines indicate the corticomedullary junction. White boxes indicate magnified areas. **$P < .01$; ***$P < .001$; ****$P < .0001$.

sjTRECs owing to their higher dilution rate, we observed a strong reduction of βTREC levels in all patients with COVID-19, although statistical significance was not reached when compared with the levels in non-ICU patients, presumably owing to the limited sample size (Fig 1, *B*). Although the ICU patient cohort of our study was very small, we found that patients who did not recover from the ICU and died had significantly lower sjTREC levels than the surviving patients (see Fig E1 in the Online Repository at www.jacionline.org).

As B-cell lymphopenia is another hallmark of COVID-19,[44,45] we sought to investigate the possibility of B-cell neogenesis defects in patients through the quantification of KRECs. We quantified sjKRECs and cjKRECs, which reflect newly generated and total B cells, respectively.[40] In agreement with previous reports,[46] we observed no differences in terms of total B-cell levels in patients with COVID-19, as measured by cjKREC quantification (Fig 1, C). However, we found reduced levels of newly generated B cells in patients, although these effects were primarily restricted to the ICU cohort (Fig 1, D). Taken together, these data suggest that SARS-CoV-2 infection affects both T- and B-cell generation, with more dramatic effects on the T-cell compartment.

Importantly, sjTREC and sjKREC levels normalized by the number of lymphocytes still show a significant drop in sjTREC and sjKREC levels in ICU patients when compared with the levels in non-ICU patients (see Fig E2 in the Online Repository at www.jacionline.org), suggesting that thymic insufficiency is independent of the general lymphopenia associated with COVID-19 and that the quantification of sjTRECs and sjKRECs is a valuable tool to assess patient at risk of life-threatening disease.

In vivo SARS-CoV-2 infection of TECs

Several viruses can directly influence thymic function by infecting cells of the thymic microenvironment.[47] Thus, we analyzed the expression of the human SARS-CoV-2 receptor ACE2 in sections of thymus tissue obtained from pediatric patients undergoing cardiac corrective surgery, as well as in an adult patient with fatal COVID-19. Immunofluorescence imaging of the pediatric thymus sections showed expression of ACE2 within the thymus, mainly restricted to large cells of the stromal microenvironment (particularly in the medulla). Importantly, we observed ACE2 coexpression with CK5, a marker that is primarily restricted to the mTEC subset[48,49] (Fig 2, A and F and see Fig E3 in the Online Repository at www.jacionline.org). Scrutinizing publicly available single-cell RNA sequencing data,[50] we found that ACE2 was preferentially enriched in a particular mTEC cluster that is characterized by the expression of CK1. Consistent with these data, further analysis revealed a broad coexpression of ACE2 within the CK1^{+} cells in the thymic medulla (Fig 2, B and F). ACE2 expression was also evaluated in thymic tissue sections of an adult patient who died of COVID-19 while in the hospital. In this case, we found a greater fraction of CK5^{+} and CK1^{+} mTECs expressing ACE2 when compared with the fractions in the pediatric tissue (Fig 2, A-D and F). Interestingly, previous single-cell RNA sequencing studies in mice and humans demonstrated that the proportion of CK1^{+} mTECs increases with age, which may suggest that the frequency of ACE2^{+} mTECs may be greater in adult patients than in pediatric patients.[50,51]

To assess whether SARS-CoV-2 could infect TECs in vivo, we evaluated the presence of SPIKE protein in the thymus of the patient fatal case of COVID-19. In agreement with the ACE2 expression data, we found SPIKE expression in the medullary compartment and its coexpression with CK5 (Fig 2, E). Taken together, these data demonstrate that the thymic epithelium is a direct target of SARS-CoV-2 infection in humans.
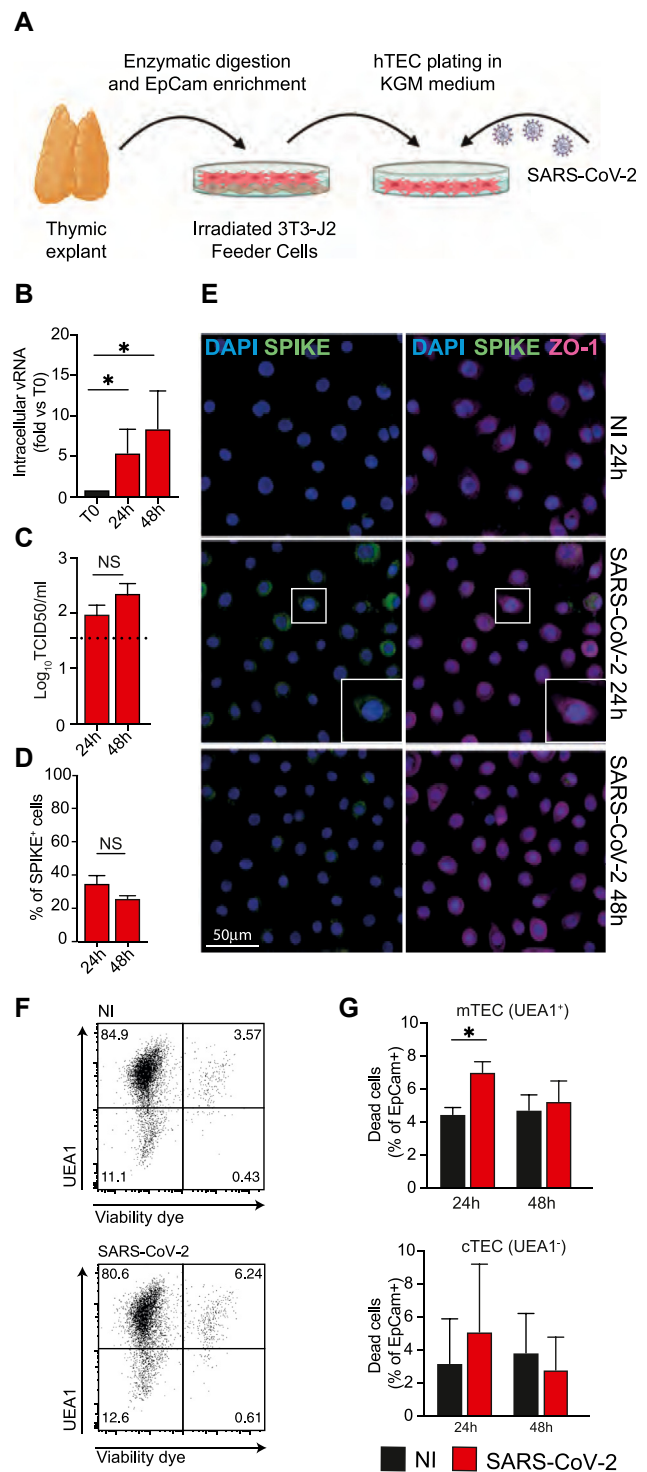
FIG 3. SARS-CoV-2 efficiently infects hTECs in vitro. **A,** Establishment of an in vitro model of primary human TEC infection with SARS-CoV-2. **B,** Viral RNA quantification in infected hTECs. Data are representative of 5 independent experiments performed with 5 biologic replicates. **C,** Released viral particles' infectious titer (median tissue culture infective dose [TCID$_{50}$]) at 24 and 48 hours after hTECs infection. **D,** Quantification of SPIKE and Zonula occludens-1 (ZO-1) colocalization in SARS-CoV-2–infected hTECs. **E,** Intracellular SARS-CoV-2 detection following hTEC infection. ZO-1 was used as an epithelial cell marker. Image representative of 2 independent experiments. **F,** Flow cytometry gating strategy to assess cell viability of the mTEC (UEA1$^+$) and cTEC (UEA1$^-$) subsets gated on EpCam-positive cells. **G,** Quantification of cell mortality within mTEC and cTEC subsets expressed as frequency of EpCam-positive cells. *$P < .05$. NS, Not significant.

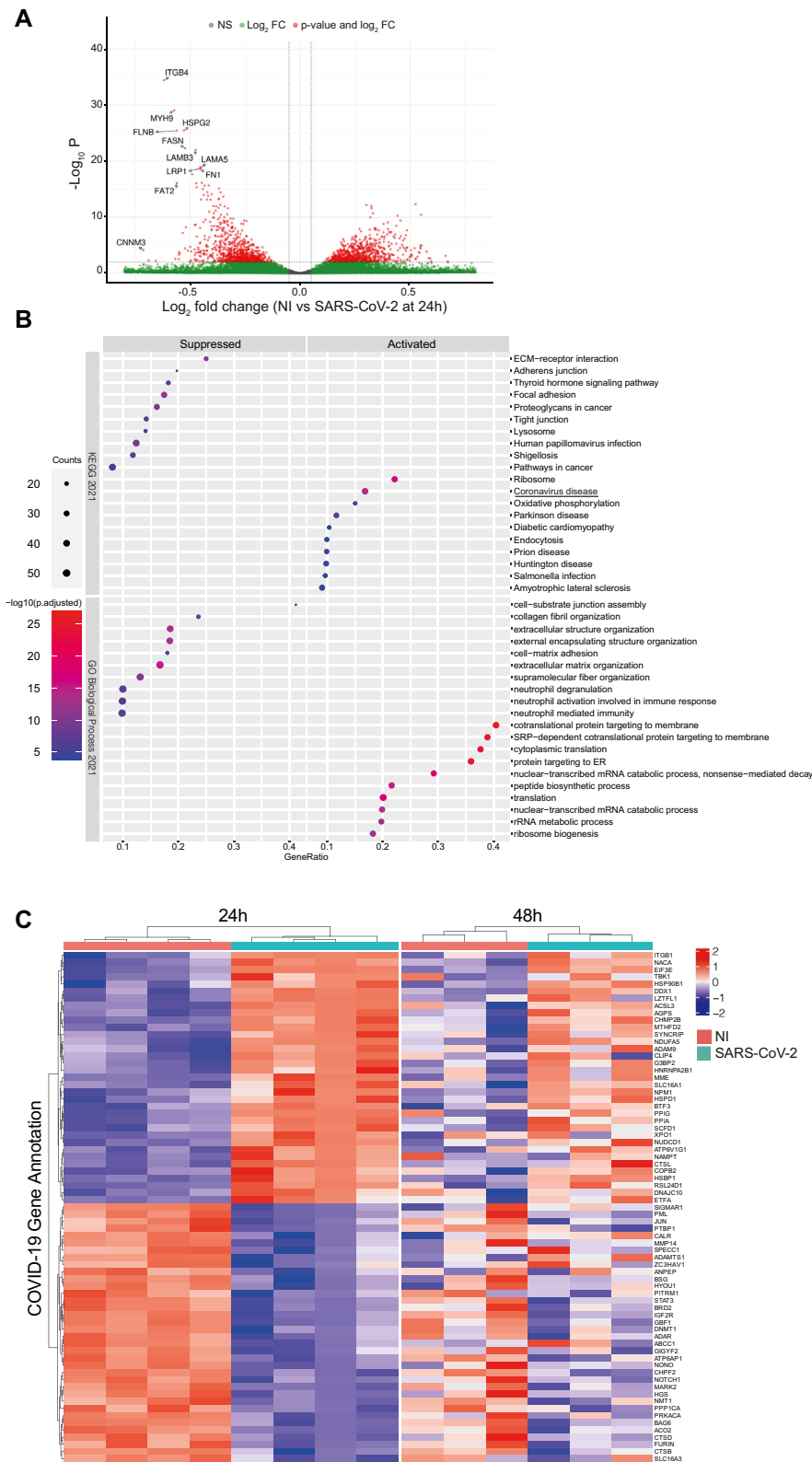**FIG 4.** Altered gene expression in hTECs after SARS-CoV-2 infection. **A**, Volcano plot showing the 1588 DEGs in hTECs 24 hours following SARS-CoV-2 infection. **B**, Kyoto Encyclopedia of Genes and Genomes pathway and Gene Ontology biologic processes enrichment analysis of DEGs. The top 10 pathways are shown; the complete list is provided in Table E1. A double scale of size and color is applied for the counts and the level of significance of the gene set enrichment, respectively. **C**, Heatmap showing the 70 protein-coding genes involved in the response to COVID-19 (Gencode annotation) found significantly ($P_{adjusted}$ <.05) deregulated in hTECs at 24 hours after infection. In parallel, the expression levels of the same genes at 48 hours after infection are also shown. Gene expression values are shown as z scores of variance stabilized data (vsd)-normalized counts, and hierarchic clustering of genes and samples was applied to highlight clusters of coregulated genes and samples with similar gene expression signatures. *ECM*, Extracellular matrix; *ER*, endoplasmic reticulum; *FC*, fold change; *NI*, not infected; *NS*, not significant.

In vitro SARS-CoV-2 infection of primary human TECs

To study the impact of SARS-CoV-2 infection on TEC function, we developed a system for *in vitro* culture of primary hTECs (Fig 3, *A*). We isolated and cultured hTECs from the thymus of pediatric individuals, and *ACE2* expression was verified trough quantitative PCR (see Fig E4, *A* in the Online Repository at www.jacionline.org). hTECs were therefore infected *in vitro* with SARS-CoV-2, and viral replication was measured at 24 and 48 hours after infection. Specifically, the replication capability of SARS-CoV-2 was evaluated by comparing viral RNA associated with hTECs as well as by measuring the infective titers of the viral particles shed by hTECs *in vitro*. An increase in cell-associated SARS-CoV-2 RNA levels was detected in hTECs after 24 hours and to a similar extent at 48 hours after infection (Fig 3, *B*). The same profile was observed when measuring the infectious titer (median tissue culture infective dose) of viral particles, suggesting that hTECs can be infected but fail to sustain an active viral replication over time (Fig 3, *C*). These data were confirmed by immunofluorescence staining, which showed SPIKE-positive hTECs at 24 and 48 hours after infection (Fig 3, *D-E*).

To further investigate the impact of SARS-CoV-2 infection on hTECs, we evaluated the proportion of medullary and cortical hTECs as well as their viability after infection. Although no significant differences in the proportion of medullary and cortical hTECs were observed (see Fig E4, *B*), we found increased mortality in the mTEC subset 24 hours after infection (Fig 3, *F-G*). This observation appears consistent with the higher ACE2 and SPIKE levels positivity observed *in vivo* in the medulla. Taken together, these data demonstrate that hTECs can be efficiently infected *in vitro*, although failing to sustain active viral replication over time.

SARS-CoV-2 infection affects gene expression in primary human TECs

To explore the biologic effects induced by SARS-CoV-2 on thymic epithelium, we evaluated the gene expression profile of hTECs after infection. The expression profiles of differentially expressed genes (DEGs) 24 hours after infection were compared with those in noninfected hTECs, revealing 1588 differentially modulated genes after SARS-CoV-2 infection: 760 genes were upregulated, whereas 828 downregulated (Fig 4, *A*). A large proportion of these genes maintained a similar differential expression at 48 hours after infection (see Fig E5, *A-D* in the Online Repository at www.jacionline.org). Of note, we found significant enrichment of sequenced reads that mapped against the reference viral genome obtained from University of California Santa Cruz database at 24 hours and 48 hours after infection, which further suggests a persistent hTEC infection *in vitro* over time (see Fig E6, *A* in the Online Repository at www.jacionline.org). Among DEGs, genes such as *ITGB4, HSPG2, LAMB3, LAMA5,* and *FN1,* which play a critical role for the maintenance of the epithelium junctions and integrity, were among the top downregulated genes after infection (Fig 4, *A*). In addition, other negatively regulated genes such as *FASN, FLNB, RRBP1, MYH9, HSPG2,* and *DYNC1H1* have recently been proposed as putative autoantigens and possibly linked to autoimmunity in patients with COVID-19.[52] The expression of top 3 downregulated genes was confirmed through quantitative PCR in nonsequenced RNA samples of infected hTECs (see Fig E6, *B*).

Next, we evaluated the expression of a discreate list of genes associated with TEC development and function. We found that the infection led to the downregulation of genes critically involved in TEC development and differentiation, such as *LTBR, RELA, NOTCH1,* and *EGFR* (see Fig E6, *C*). On the other hand, SARS-CoV-2 infection induced the expression of *CTSL* and *ATG5*. Interestingly, *CTSL* (cathepsin 1) has been recently shown to be upregulated after SARS-CoV-2 infection.[53] As the expression of peripheral tissue–restricted antigens by TECs is critical to establish central tolerance to self, we further searched for known autoantigens differentially regulated after hTEC infection. Interestingly, we found that the tissue autoantigen *SOX9,* expression of which is predominantly restricted to skin, was significantly downregulated after SARS-CoV-2 infection.[13] Although our data on the expression of autoantigens were limited, our study suggests that along with causing transcriptional changes of genes important for TEC maintenance, SARS-CoV-2 infection might also negatively regulate the expression of potential tissue-restricted antigens.

Subsequentially, to gain insights into the biologic pathways affected by SARS-CoV-2 infection, we performed Gene Ontology (GO) classifications and Kyoto Encyclopedia of Genes and Genomes pathway analyses of DEGs. The Kyoto Encyclopedia of Genes and Genomes analysis showed enrichment of different pathways, including the coronavirus disease pathway, indicating that infected TECs showed transcriptome status in line with that shown by other coronavirus-infected cell types (Fig 4, *B*). Our analysis further showed that SARS-CoV-2 infection regulated critical processes related to cellular metabolism. In particular, we found that oxidative phosphorylation was among the top 3 activated pathways following infection (Fig 4, *B*). In addition, the tricarboxylic acid cycle was also significantly increased in SARS-CoV-2–infected hTECs (see Table E1 in the Online Repository at www.jacionline.org). On the other hand, pathways involved in focal adhesion and extracellular matrix interaction, which play a critical role in epithelial cell maintenance, adhesion, and survival, were significantly downregulated after infection.

To further investigate the perturbation in gene expression induced by SARS-CoV-2 infection, we compared the DEGs with the Gencode COVID-19 Gene Annotation, a public set of human protein–coding genes linked to SARS-CoV-2 infection. Among the 321 genes currently validated in the gene set, 70 matched with the DEGs that we observed in infected hTECs (36 downregulated and 34 upregulated) (Fig 4, *C*) and 63 maintained similar gene expression changes at 48 hours after infection. To better understand the biologic pathways affected by SARS-CoV-2 infection, we used Gene Ontology for functional annotation and tested the enrichment of coronavirus disease–associated DEGs; we observed the activation of pathways associated with virus entry into a host cell (*CTSL* and *PPIA* genes), whereas many of the downregulated genes were strongly associated with proteolysis and cell cycle regulation (see Fig E6, *D*). Taken together, these results demonstrate that SARS-CoV-2 infection has a profound impact on gene expression of human TECs, negatively regulating pathways critical for TEC maintenance and inducing transcriptional changes consistent with the COVID-19 gene signature.

DISCUSSION

Since its emergence in December 2019, SARS-CoV-2 has quickly spread across the globe. The virus exploits ACE2 as the primary cell entry receptor, and its infection leads to the highly infective COVID-19. Given the complexity of the disease and the surge of viral variants with high fatality risk, it is paramount to comprehensively characterize the effects of the virus on its biologic targets to develop effective treatments against COVID-19 and identify patients at risk of severe disease.

Clinically, COVID-19 is associated with a broad spectrum of symptoms and complications. Although a large body of literature has investigated the effects of the infection on lymphopenia, very few studies have assessed whether the process of T-cell and B-cell lymphopoiesis is altered in patients with COVID-19. Here we present for the first time evidence that the thymus is a target of SARS-CoV-2 infection *in vivo* and that thymic function is impaired in patients with COVID-19. We first demonstrated that patients with COVID-19 display decreased levels of TRECs and KRECs, which represent surrogate markers of T- and B-cell neogenesis, respectively. Moreover, our data demonstrated a more severe reduction in TREC levels in both non-ICU and ICU patients, whereas KRECs were less affected. These results are in agreement with previously published data showing that the T-cell pool is more affected during COVID-19 than the B-cell compartment is.[46,54] Given these results, we sought to investigate a possible direct impact of SARS-CoV-2 on the thymus. Our data demonstrated that thymic epithelium of pediatric and adult patients expresses the SARS-CoV-2 receptor ACE2 and that SARS-CoV-2 entry into the cells resulted in fundamental changes in gene expression profile. Our data suggest that following infection, SARS-CoV-2 recruits a variety of host factors to survive and propagate itself, as suggested by the activation of different pathways associated with ribosome biogenesis and protein translation. These effects are associated with the derangement of the normal gene expression profile in TECs, leading to the downregulation of crucial pathways involved in epithelium cell maintenance (such as focal adhesion and extracellular matrix interaction) and upregulation of metabolic processes (such as oxidative phosphorylation). The activation of these metabolic pathways may result in the rise of oxidative stress, which could explain the decrease in vitality and increase in mitophagy pathway observed in SARS-CoV-2–infected cells (see Table E1). Although we showed that primary hTECs were unable to sustain effective viral replication in an *in vitro* culture system (which is a finding observed in other cellular systems[55,56]), our data demonstrate that SARS-CoV-2 can persist in infected hTECs over time *in vitro* and *in vivo*. Thus, along with the changes induced by the direct infection of cells, recirculating virus-specific T cells could target infected TECs and significantly contribute to thymic damage and reduced thymic output. Previous studies conducted on mouse models of mycobacterial and lymphocytic choriomeningitis virus (LCMV) infections support this hypothesis.[57,58]

Impaired thymic function in patients with COVID-19 could potentially lead to significant immunologic consequences. In addition to its vital importance in generating the T-cell pool during early life, optimal thymic function is required to reestablish T-cell immunity after periods of immunologic insults, such as those caused by antineoplastic therapies, immunosuppressive treatments, and infections. Reduced thymic function and the resulting decrease in T-cell export could exacerbate lymphopenia

in acutely ill patients with COVID-19 and increase the time required to restore the number and function of circulating T-cells after recovery. Delayed recovery of thymic function may contribute to the development of secondary infections, which can worsen the severity of the illness, increase the risk of disease progression,[59] and facilitate persistent symptoms associated with herpesvirus reactivation.[60] Furthermore, the direct impact of SARS-CoV-2 on TECs and the additional damage caused by the rise in proinflammatory molecules, such as interferons, IL-6, and TNF-α, which have all been implicated in acute thymic involution,[61] could lead to suboptimal education of the developing thymocytes. An impaired process of T-cell development might alter the process of central tolerance and generate the maturation of T-cell responses to self-antigens that lead to the development of autoimmune response against self-tissue antigens. The relationship between viral infections and the development of autoimmune diseases, such as multiple sclerosis, rheumatoid arthritis, type 1 diabetes, and SLE, is well known.[62] However, the underlying mechanisms of this association are still largely unexplored, although evidence suggests that molecular mimicry, bystander T-cell activation, and abnormal nucleic acid sensing may play a role.[63,64] Breaching of central tolerance has been also proposed. Several viruses, including HIV, measles virus, LCMV, yellow fever virus, and Zika virus, can cause thymic involution and altered thymic epithelium architecture and function.[20,24,28,57,65,66] Recent evidence in mouse models of roseolovirus and LCMV infections demonstrated a direct link between viral infection and the development of autoimmunity[67] and self-reactive T cells.[57] SARS-CoV-2 infection generates a strong and excessive inflammatory response involving pathways and targets known to be commonly associated with autoimmune and inflammatory diseases. Whether SARS-CoV-2 induces or exacerbates autoimmunity is an active area of research, particularly now that several reports on a potential association of COVID-19 with autoimmune diseases (such as idiopathic thrombocytopenic purpura, multisystem inflammatory syndrome in children, autoimmune thyroid disease, and Guillain–Barré syndrome) have gradually started to emerge.[68]

Lastly, studies in experimental mouse models have demonstrated that infections of the thymic microenvironment results in the emergence of pathogen-specific tolerance, as shown for LCMV, murine leukemia virus,[69] hepatitis B virus,[69] and *Mycobacterium avium* infections.[70] However, whether this is relevant in human infections is a matter of investigation.

To the best of our knowledge, our studies are unique in establishing that SARS-CoV-2 can directly target the thymus and alter gene expression profile of thymic epithelium. We propose that the evaluation of thymic functionality (eg, by quantifying sjTRECs in patient peripheral blood) may be a useful marker to identify patients with COVID-19 at risk of complication both in acute and convalescent phases. Although the data that we have collected on altered expression of potential autoantigens are limited, our study also raises the possibility that disruption of thymic function by SARS-CoV-2 may be an additional mechanism to explain the excessive inflammation and potentially contribute to the development of autoimmune diseases related to COVID-19.

> **Clinical implications: Patients with COVID-19 have reduced thymic T-cell output, and disease severity is inversely correlated with thymic function. Monitoring thymic activity may be a useful marker to evaluate disease severity and progression.**

REFERENCES

1. Tavakolpour S, Rakhshandehroo T, Wei EX, Rashidian M. Lymphopenia during the COVID-19 infection: what it shows and what can be learned. Immunol Lett 2020;225:31-2.
2. Tan L, Wang Q, Zhang D, Ding J, Huang Q, Tang YQ, et al. Lymphopenia predicts disease severity of COVID-19: a descriptive and predictive study. Signal Transduct Targ Ther 2020;5:33.
3. Chen G, Wu D, Guo W, Cao Y, Huang D, Wang H, et al. Clinical and immunological features of severe and moderate coronavirus disease 2019. J Clin Invest 2020; 130:2620-9.
4. Mathew D, Giles JR, Baxter AE, Greenplate AR, Wu JE, Alanio C, et al. Deep immune profiling of COVID-19 patients reveals patient heterogeneity and distinct immunotypes with implications for therapeutic interventions. bioRxiv 2020; https://doi.org/10.1101/2020.05.20.106401.
5. Lucas C, Wong P, Klein J, Castro TBR, Silva J, Sundaram M, et al. Longitudinal analyses reveal immunological misfiring in severe COVID-19. Nature 2020;584: 463-9.
6. Chu H, Zhou J, Wong BHY, Li C, Chan JFW, Cheng ZS, et al. Middle East respiratory syndrome coronavirus efficiently infects human primary T lymphocytes and activates the extrinsic and intrinsic apoptosis pathways. J Infect Dis 2016;213:904-14.
7. Bordoni V, Tartaglia E, Sacchi A, Fimia GM, Cimini E, Casetti R, et al. The unbalanced p53/SIRT1 axis may impact lymphocyte homeostasis in COVID-19 patients. Int J Infect Dis 2021;105:49-53.
8. Song JW, Zhang C, Fan X, Meng FP, Xu Z, Xia P, et al. Immunological and inflammatory profiles in mild and severe cases of COVID-19. Nat Commun 2020;11: 3410.
9. Han J, Zúñiga-Pflücker JCA. 2020 view of thymus stromal cells in T cell development. J Immunol 2021;206:249-56.
10. Takahama Y. Journey through the thymus: stromal guides for T-cell development and selection. Nat Rev Immunol 2006;6:127-35.
11. Petrie HT, Zúñiga-Pflücker JC. Zoned out: functional mapping of stromal signaling microenvironments in the thymus. Annu Rev Immunol 2007;25:649-79.
12. Kadouri N, Nevo S, Goldfarb Y, Abramson J. Thymic epithelial cell heterogeneity: TEC by TEC. Nat Rev Immunol 2020;20:239-53.
13. Sansom SN, Shikama-Dorn N, Zhanybekova S, Nusspaumer G, Macaulay IC, Deadman ME, et al. Population and single-cell genomics reveal the Aire dependency, relief from Polycomb silencing, and distribution of self-antigen expression in thymic epithelia. Genome Res 2014;24:1918-31.
14. Velardi E, Tsai JJ, van den Brink MRM. T cell regeneration after immunological injury. Nat Rev Immunol 2021;21:277-91.
15. Majumdar S, Deobagkar-Lele M, Adiga V, Raghavan A, Wadhwa N, Ahmed SM, et al. Differential susceptibility and maturation of thymocyte subsets during Salmonella Ttyphimurium infection: insights on the roles of glucocorticoids and interferon-gamma. Sci Rep 2017;7:40793.
16. Ferrando-Martinez S, De Pablo-Bernal RS, De Luna-Romero M, De Ory SJ, Genebat M, Pacheco YM, et al. Thymic function failure is associated with human immunodeficiency virus disease progression. Clin Infect Dis 2017;64:1191-7.
17. Rosado-Sánchez I, Herrero-Fernández I, Genebat M, Ruiz-Mateos E, Leal M, Pacheco YM. Thymic function impacts the peripheral CD4/CD8 ratio of HIV-infected subjects. Clin Infect Dis 2017;64:152-8.
18. Fiume G, Scialdone A, Albano F, Rossi A, Maria Tuccillo F, Rea D, et al. Impairment of T cell development and acute inflammatory response in HIV-1 Tat transgenic mice. Sci Rep 2015;5:13864.
19. Hartling HJ, Gaardbo JC, Ronit A, Salem M, Laye M, Clausen MR, et al. Impaired thymic output in patients with chronic hepatitis C virus infection. Scand J Immunol 2013;78:378-86.
20. Autran B, Guiet P, Raphael M, Grandadam M, Agut H, Candotti D, et al. Thymocyte and thymic microenvironment alterations during a systemic HIV infection in a severe combined immunodeficient mouse model. AIDS 1996;10:717-27.
21. Douek DC, Betts MR, Hill BJ, Little SJ, Lempicki R, Metcalf JA, et al. Evidence for increased T cell turnover and decreased thymic output in HIV infection. J Immunol 2001;167:6663.
22. Stanley SK, McCune JM, Kaneshima H, Justement JS, Sullivan M, Boone E, et al. Human immunodeficiency virus infection of the human thymus and disruption of the thymic microenvironment in the SCID-hu mouse. J Exp Med 1993;178:1151-63.
23. Braun J, Valentin H, Nugeyre MT, Ohayon H, Gounon P, Barré-Sinoussi F. Productive and persistent infection of human thymic epithelial cells in vitro with HIV-1. Virology 1996;225:413-8.
24. Valentin H, Azocar O, Horvat B, Williems R, Garrone R, Evlashev A, et al. Measles virus infection induces terminal differentiation of human thymic epithelial cells. J Virol 1999;73:2212.
25. Numazaki K, Goldman H, Wong I, Wainberg MA. Replication of measles virus in cultured human thymic epithelial cells. J Med Virol 1989;27:52-8.
26. Maguer-Satta V, Gazzolo L, Dodon MD. Human immature thymocytes as target cells of the leukemogenic activity of human T-cell leukemia virus type I. Blood 1995;86:1444-52.
27. Manca N, Perandin F, De Simone N, Giannini F, Bonifati D, Angelini C. Detection of HTLV-I tax-rex and pol gene sequences of thymus gland in a large group of patients with myasthenia gravis. J Acquir Immune Defic Syndr 2002;29:300-6.
28. Messias CV, Loss-Morais G, Carvalho JB de, González MN, Cunha DP, Vasconcelos Z, et al. Zika virus targets the human thymic epithelium. Sci Rep 2020;10:1-17.
29. Vogel AB, Haasbach E, Reiling SJ, Droebner K, Klingel K, Planz O. Highly pathogenic influenza virus infection of the thymus interferes with T lymphocyte development. J Immunol 2010;185:4824-34.
30. Wykrzykowska JJ, Rosenzweig M, Veazey RS, Simon MA, Halvorsen K, Desrosiers RC, et al. Early regeneration of thymic progenitors in rhesus macaques infected with simian immunodeficiency virus. J Exp Med 1998;187:1767-78.
31. Cuvelier P, Roux H, Couëdel-Courteille A, Dutrieux J, Naudin C, Charmeteau de Muylder B, et al. Protective reactive thymus hyperplasia in COVID-19 acute respiratory distress syndrome. Crit Care 2021;25:4.
32. Savchenko AA, Tikhonova E, Kudryavtsev I, Kudlay D, Korsunsky I, Beleniuk V, et al. TREC/KREC levels and T and B lymphocyte subpopulations in COVID-19 patients at different stages of the disease. Viruses 2022;14:646.
33. Green H, Kehinde O, Thomas J. Growth of cultured human epidermal cells into multiple epithelia suitable for grafting. Proc Natl Acad Sci U S A 1979;76:5665-8.
34. Wang Z, Xu X. scRNA-seq profiling of human testes reveals the presence of the ACE2 receptor, a target for SARS-CoV-2 infection in spermatogonia, Leydig and Sertoli cells. Cells 2020;9:920.
35. Chen S, Zhou Y, Chen Y, Gu J. fastp: an ultra-fast all-in-one FASTQ preprocessor. Bioinformatics 2018;34:i884-90.
36. Dobin A, Davis CA, Schlesinger F, Drenkow J, Zaleski C, Jha S, et al. STAR: ultrafast universal RNA-seq aligner. Bioinformatics 2013;29:15-21.
37. Liao Y, Smyth GK, Shi W. featureCounts: an efficient general purpose program for assigning sequence reads to genomic features. Bioinformatics 2014;30:923-30.
38. Love MI, Huber W, Anders S. Moderated estimation of fold change and dispersion for RNA-seq data with DESeq2. Genome Biol 2014;15:550.
39. Ritchie ME, Phipson B, Wu D, Hu Y, Law CW, Shi W, et al. limma powers differential expression analyses for RNA-sequencing and microarray studies. Nucleic Acids Res 2015;43:e47.
40. Arruda LCM, Malmegrim KCR, Lima-Júnior JR, Clave E, Dias JBE, Moraes DA, et al. Immune rebound associates with a favorable clinical response to autologous HSCT in systemic sclerosis patients. Blood Adv 2018;2:126-41.
41. Clave E, Busson M, Douay C, De Latour RP, Berrou J, Rabian C, et al. Acute graft-versus-host disease transiently impairs thymic output in young patients after allogeneic hematopoietic stem cell transplantation. Blood 2009;113:6477-84.
42. Clave E, Rocha V, Talvensaari K, Busson M, Douay C, Appert ML, et al. Prognostic value of pretransplantation host thymic function in HLA-identical sibling hematopoietic stem cell transplantation. Blood 2005;105:2608-13.
43. Hazenberg MD, Verschuren MC, Hamann D, Miedema F, Dongen JJ. T cell receptor excision circles as markers for recent thymic emigrants: basic aspects, technical approach, and guidelines for interpretation. J Mol Med 2001;79:631-40.
44. Balzanelli MG, Distratis P, Dipalma G, Vimercati L, Catucci O, Amatulli F, et al. Immunity profiling of covid-19 infection, dynamic variations of lymphocyte subsets, a comparative analysis on four different groups. Microorganisms 2021;9:2036.
45. Chan SSW, Christopher D, Tan GB, Chong VCL, Fan BE, Lin CY, et al. Peripheral lymphocyte subset alterations in COVID-19 patients. Int J Lab Hematol 2020;42: e199-203.
46. Carsetti R, Zaffina S, Piano Mortari E, Terreri S, Corrente F, Capponi C, et al. Different innate and adaptive immune responses to SARS-CoV-2 infection of asymptomatic, mild, and severe cases. Front Immunol 2020;11:610300.
47. Kourtis AP, Ibegbu C, Nahmias AJ, Lee FK, Clark WS, Sawyer MK, et al. Early progression of disease in HIV-infected infants with thymus dysfunction. N Engl J Med 1996;335:1431-6.
48. Alexandropoulos K, Danzl NM. Thymic epithelial cells: antigen presenting cells that regulate T cell repertoire and tolerance development. Immunol Res 2012;54: 177-90.

49. Li J, Gordon J, Chen ELY, Xiao S, Wu L, Zúniga-Pflücker JC, et al. NOTCH1 signaling establishes the medullary thymic epithelial cell progenitor pool during mouse fetal development. Dev 2020;147:1-15.

50. Park JE, Botting RA, Conde CD, Popescu DM, Lavaert M, Kunz DJ, et al. A cell atlas of human thymic development defines T cell repertoire formation. Science 2020;367:eaay3224.

51. Bornstein C, Nevo S, Giladi A, Kadouri N, Pouzolles M, Gerbe F, et al. Single-cell mapping of the thymic stroma identifies IL-25-producing tuft epithelial cells. Nature 2018;559:622-6.

52. Wang JY, Roehrl MW, Roehrl VB, Roehrl MH. A master autoantigen-ome links alternative splicing, female predilection, and COVID-19 to autoimmune diseases. J Transl Autoimmun 2022;5:100147.

53. Zhao MM, Yang WL, Yang FY, Zhang L, Huang WJ, Hou W, et al. Cathepsin L plays a key role in SARS-CoV-2 infection in humans and humanized mice and is a promising target for new drug development. Signal Transduct Target Ther 2021;6:134.

54. Weiskopf D, Schmitz KS, Raadsen MP, Grifoni A, Okba NMA, Endeman H, et al. Phenotype and kinetics of SARS-CoV-2-specific T cells in COVID-19 patients with acute respiratory distress syndrome. Sci Immunol 2020;5:eabd2071.

55. Bordoni V, Mariotti D, Matusali G, Colavita F, Cimini E, Ippolito G, et al. SARS-CoV-2 infection of airway epithelium triggers pulmonary endothelial cell activation and senescence associated with type I IFN production. Cells 2022;11:2912.

56. Wurtz N, Penant G, Jardot P, Duclos N, La Scola B. Culture of SARS-CoV-2 in a panel of laboratory cell lines, permissivity, and differences in growth profile. Eur J Clin Microbiol Infect Dis 2021;40:477-84.

57. Elsaesser HJ, Mohtashami M, Osokine I, Snell LM, Cunningham CR, Boukhaled GM, et al. Chronic virus infection drives CD8 T cell-mediated thymic destruction and impaired negative selection. Proc Natl Acad Sci U S A 2020; 117:5420-9.

58. Nobrega C, Nunes-Alves C, Cerqueira-Rodrigues B, Roque S, Barreira-Silva P, Behar SM, et al. T Cells home to the thymus and control infection. J Immunol 2013; 190:1646-58.

59. De Bruyn A, Verellen S, Bruckers L, Geebelen L, Callebaut I, De Pauw I, et al. Secondary infection in COVID-19 critically ill patients: a retrospective single-center evaluation. BMC Infect Dis 2022;22:1-7.

60. Gold JE, Okyay RA, Licht WE, Hurley DJ. Investigation of long COVID prevalence and its relationship to epstein-barr virus reactivation. Pathogens 2021;10:763.

61. Ansari AR, Liu H. Acute thymic involution and mechanisms for recovery. Arch Immunol Ther Exp 2017;65:401-20.

62. Smatti MK, Cyprian FS, Nasrallah GK, Al Thani AA, Almishal RO, Yassine HM. Viruses and autoimmunity: a review on the potential interaction and molecular mechanisms. Viruses 2019;11:762.

63. Fujinami RS, Oldstone MBA. Amino acid homology between the encephalitogenic site of myelin basic protein and virus: mechanism for autoimmunity. Science 1985; 230:1043-5.

64. Münz C, Lünemann JD, Getts MT, Miller SD. Antiviral immune responses: triggers of or triggered by autoimmunity? Nat Rev Immunol 2009;9:246-58.

65. Melo-Lima BL, Espósito DLA, Fonseca BAL Da, Figueiredo LTM, Moreau P, Donadi EA. The attenuated live yellow fever virus 17D infects the thymus and induces thymic transcriptional modifications of immunomodulatory genes in C57BL/6 and BALB/C mice. Autoimmune Dis 2015;2015:503087.

66. Linhares-Lacerda L, Palu CC, Ribeiro-Alves M, Paredes BD, Morrot A, Garcia-Silva MR, et al. Differential expression of microRNAs in thymic epithelial cells from trypanosoma cruzi acutely infected mice: putative role in thymic atrophy. Front Immunol 2015;6:428.

67. Bigley TM, Yang L, Kang LI, Saenz JB, Victorino F, Yokoyama WM. Disruption of thymic central tolerance by infection with murine roseolovirus induces autoimmune gastritis. J Exp Med 2022;219:e20211403.

68. Icenogle T. COVID-19: Infection or autoimmunity. Front Immunol 2020;11:2055.

69. Korostoff JM, Nakada MT, Faas SJ, Blank KJ, Gaulton GN. Neonatal exposure to thymotropic gross murine leukemia virus induces virus-specific immunologic nonresponsiveness. J Exp Med 1990;172:1765-75.

70. Nobrega C, Roque S, Nunes-Alves C, Coelho A, Medeiros I, Castro AG, et al. Dissemination of Mycobacteria to the thymus renders newly generated T cells tolerant to the invading pathogen. J Immunol 2010;184:351-8.